

Supporting Information

Supramolecular Switch for the Regulation of Antibacterial Efficacy of Near-Infrared Photosensitizer

Yu-Na Jiang^{1,2}, Manqi Tan^{1,2}, Chenglong He^{1,2}, Jiaxi Wang³, Yi Wei³, Ningning Jing⁴, Bing Wang^{2,5}, Fang Yang^{1,2,5,*}, Yujie Zhang^{1,2,5,*} and Meng Li^{2,5,*}

¹ Cixi Biomedical Research Institute, Wenzhou Medical University, Ningbo 315302, China;

jiangyuna@nimte.ac.cn (Y.-N.J.); tanmanqi@nimte.ac.cn (M.T.); hechenglong@nimte.ac.cn (C.H.)

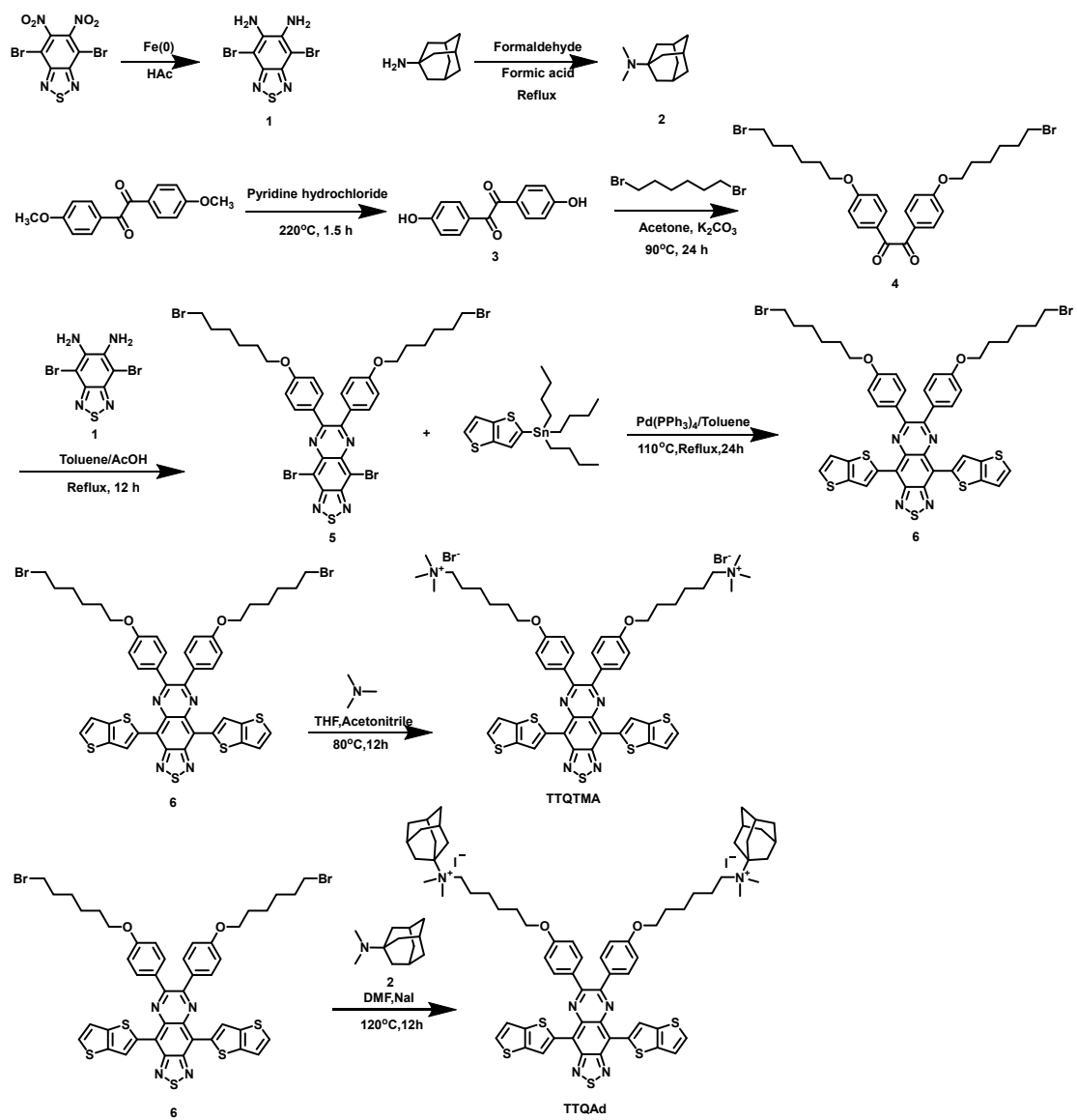
² Ningbo Key Laboratory of Biomedical Imaging Probe Materials and Technology, Ningbo Institute of Materials Technology and Engineering, Chinese Academy of Sciences, Ningbo 315201, China; wangbing@nimte.ac.cn

³ School of Materials Science and Engineering, University of Science and Technology Beijing, Beijing 100083, China; jiaxi0726@163.com (J.W.); weiyi5166@126.com (Y.W.)

⁴ College of Science and Technology, Ningbo University, Ningbo 315300, China; jingnn7009@163.com

⁵ Zhejiang International Scientific and Technological Cooperative Base of Biomedical Materials and Technology, Ningbo Cixi Institute of Biomedical Engineering, Ningbo 315300, China

* Correspondence: yangf@nimte.ac.cn (F.Y.); zhangyujie@nimte.ac.cn (Y.Z.); limeng@nimte.ac.cn (M.L.)



Scheme S1. The synthetic routes of TTQAd and TTQTMA.

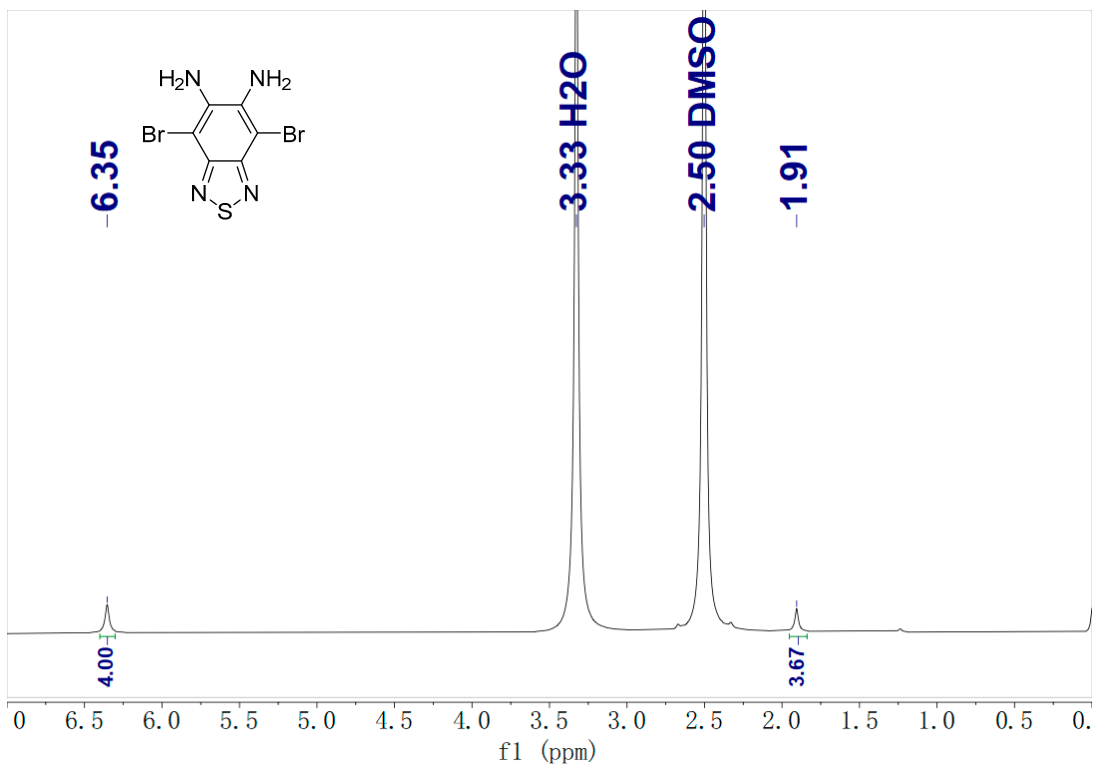


Figure S1. ^1H NMR spectrum of 4,7-dibromo-2,1,3-benzothiadiazole-5,6-diamine (1) in DMSO.

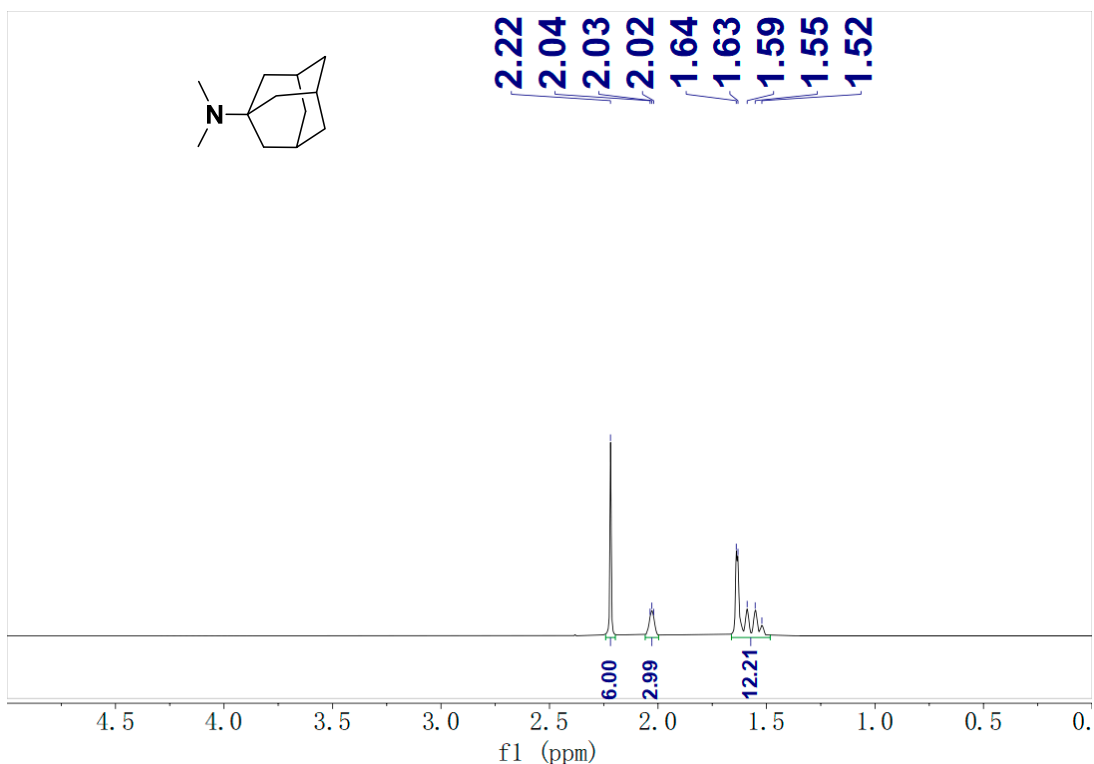


Figure S2. ^1H NMR spectrum of dimethyl-1-adamantylamine (2) in CDCl_3 .

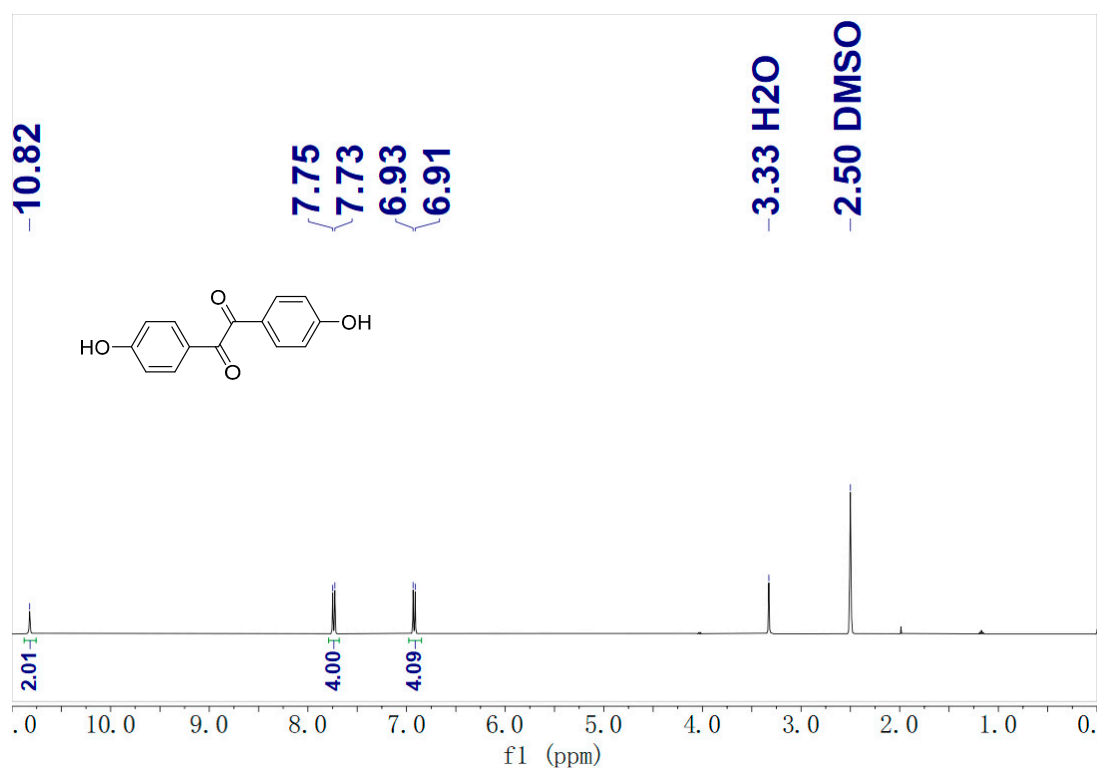


Figure S3. ^1H NMR spectrum of 4,4'-dihydroxy-benzil (3) in DMSO.

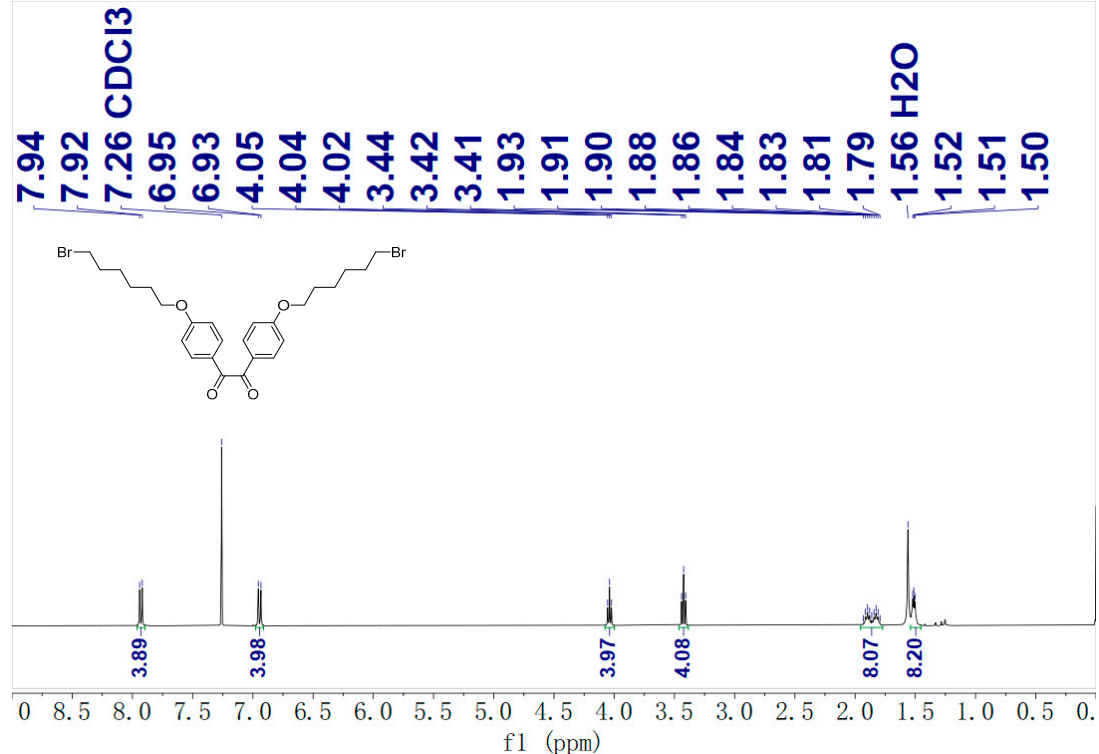


Figure S4. ^1H NMR spectrum of compound 4 in DMSO.

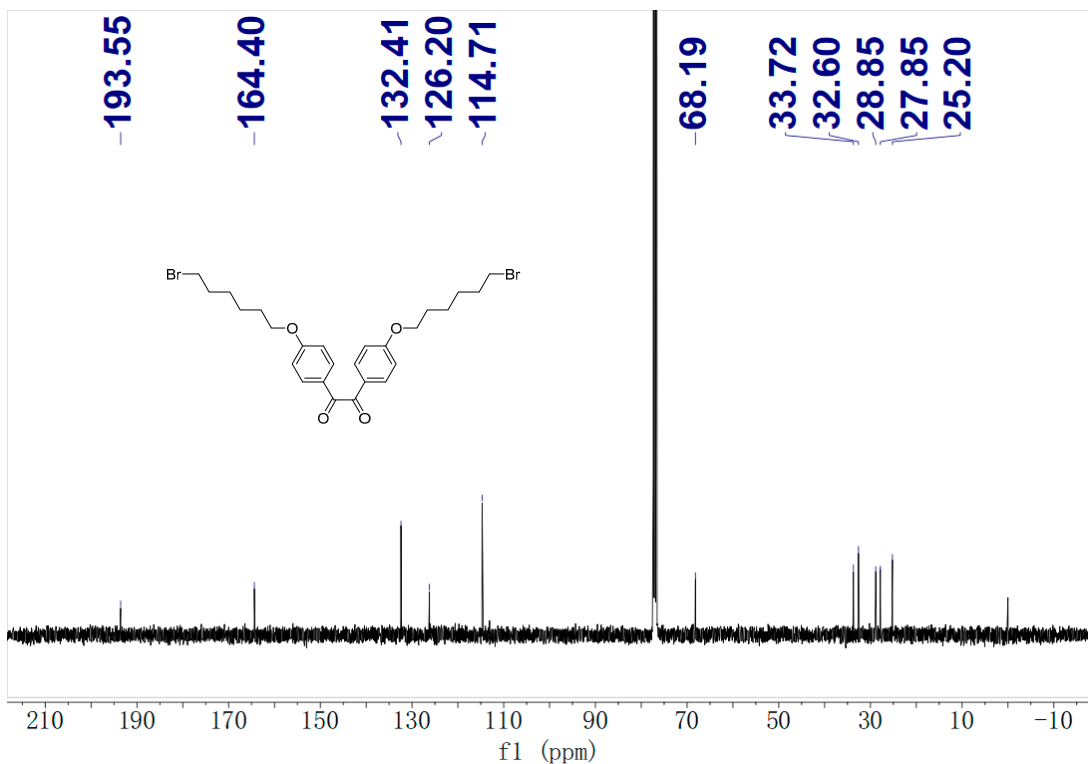


Figure S5. ^{13}C NMR spectrum of compound 4 in DMSO.

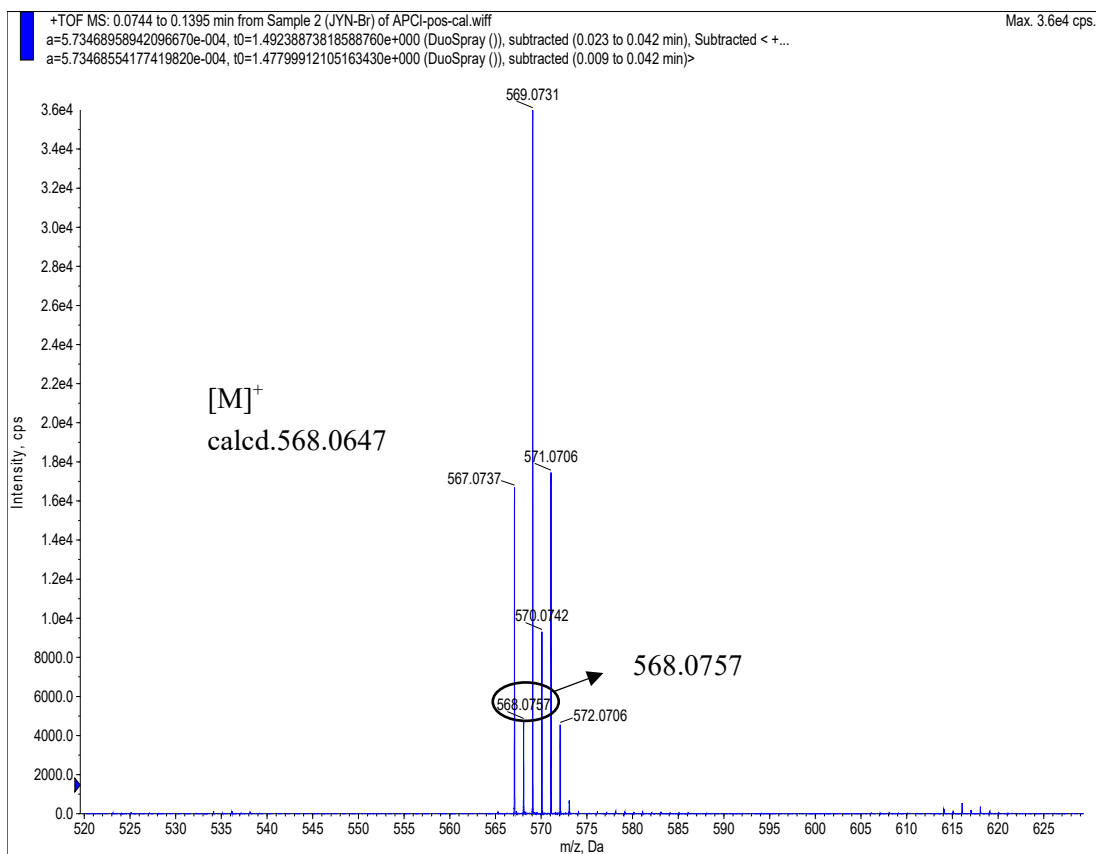


Figure S6. HRMS of Compound 4.

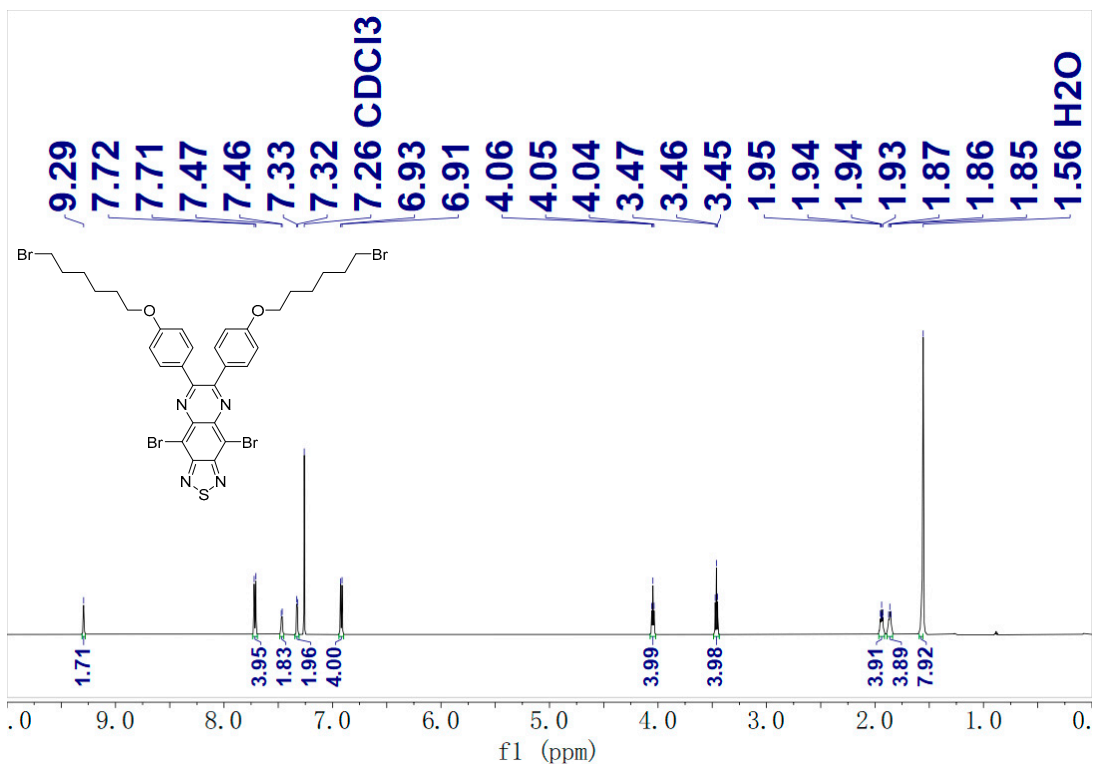


Figure S7. ^1H NMR spectrum of compound 5 in CDCl_3 .

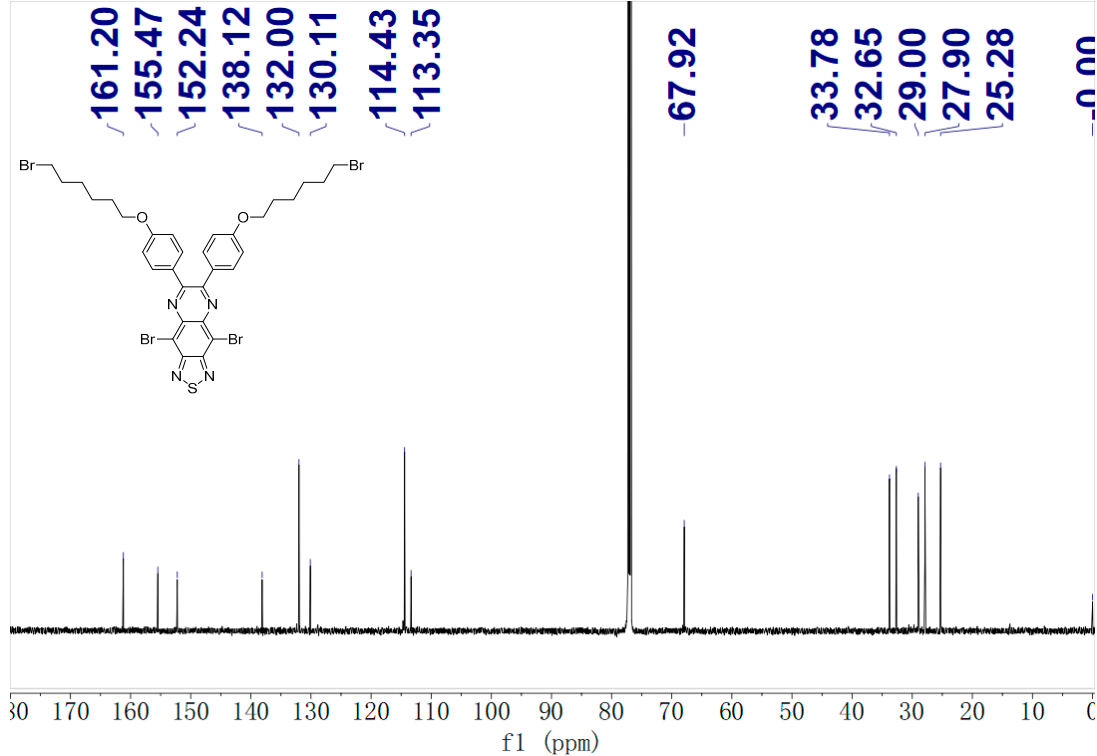


Figure S8. ^{13}C NMR spectrum of compound 5 in CDCl_3 .

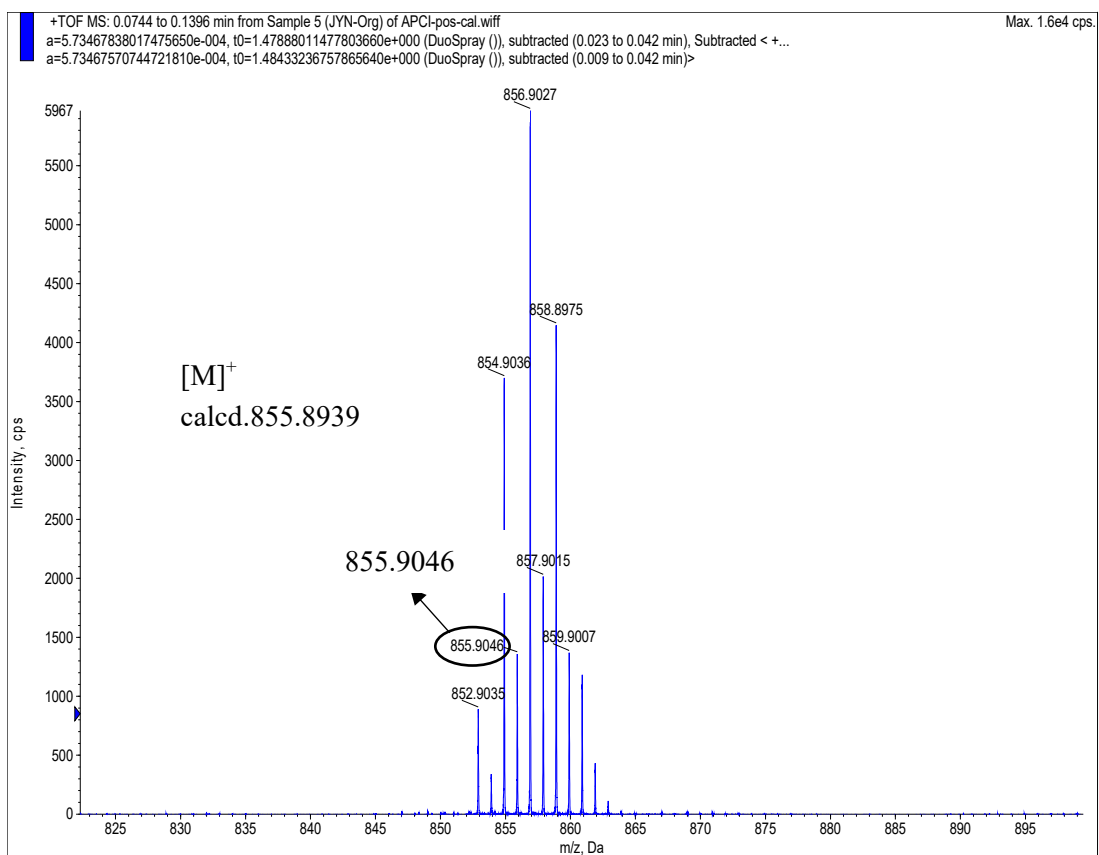


Figure S9. HRMS of compound 5.

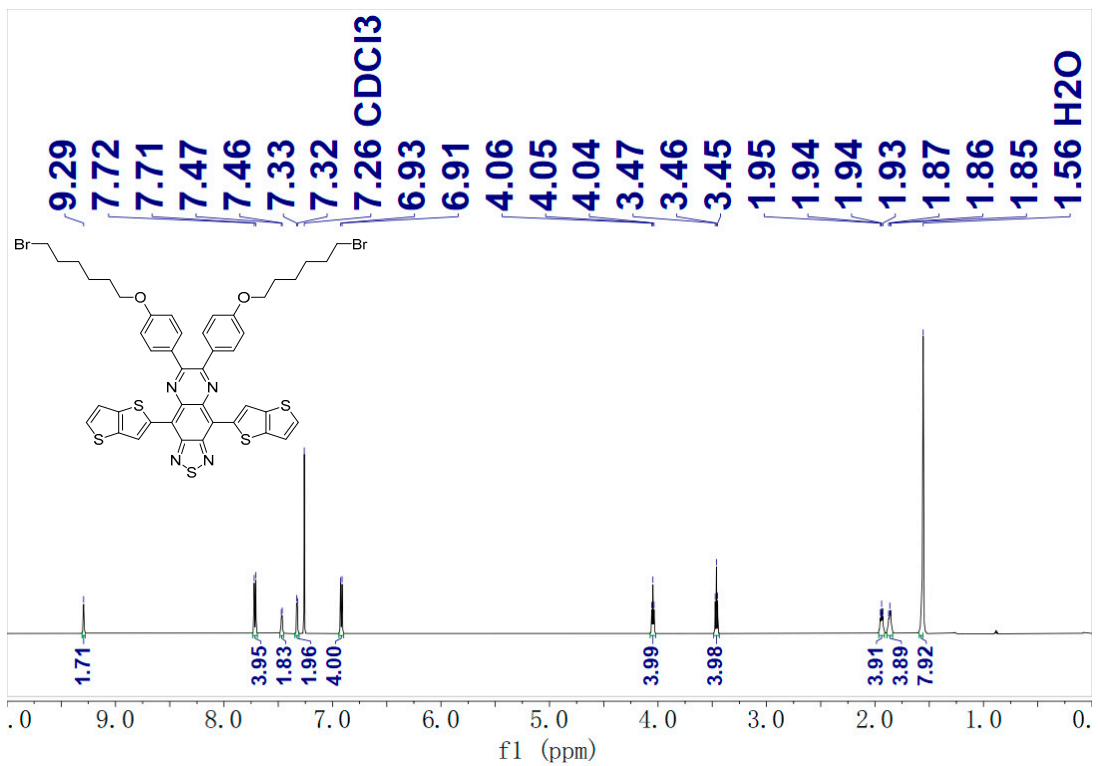


Figure S10. ^1H NMR spectrum of compound 6 in CDCl_3 .

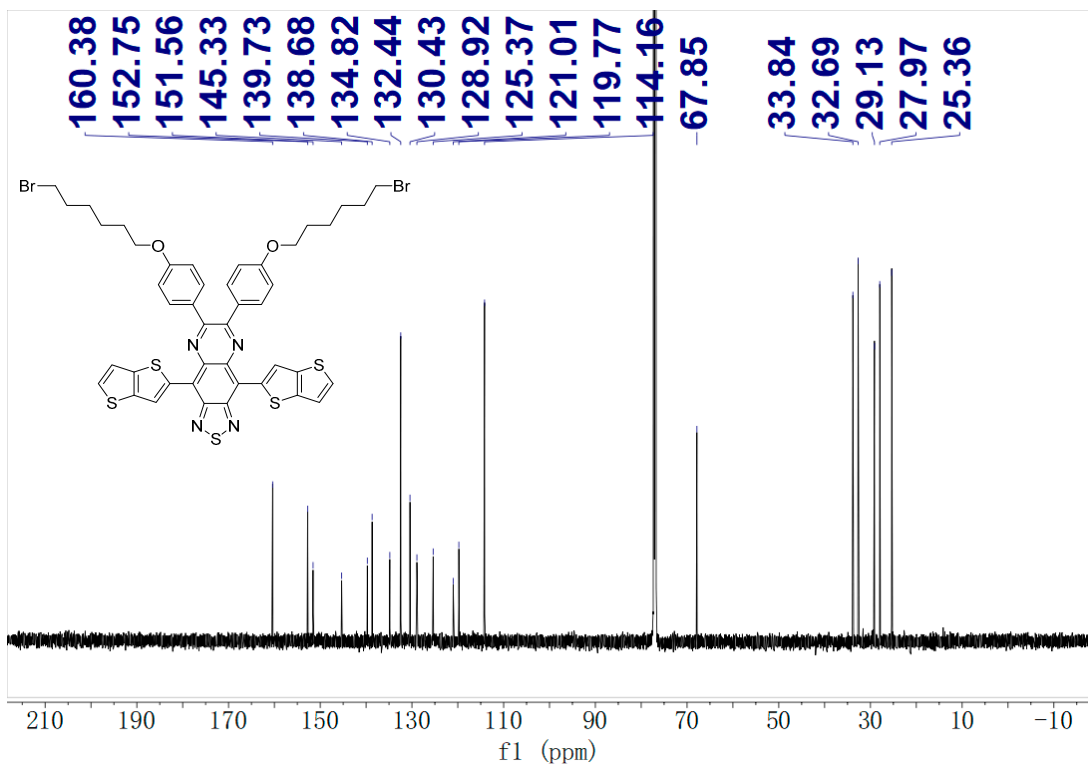


Figure S11. ^{13}C NMR spectrum of compound 6 in CDCl_3 .

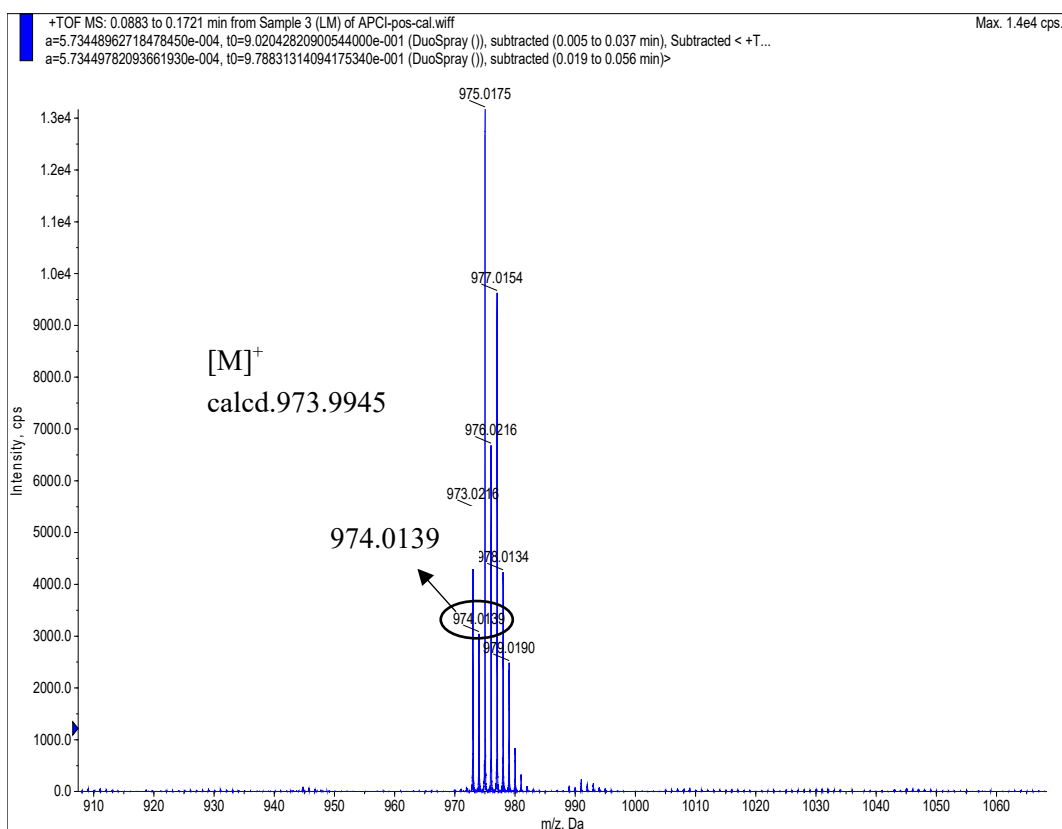


Figure S12. HRMS of compound 6.

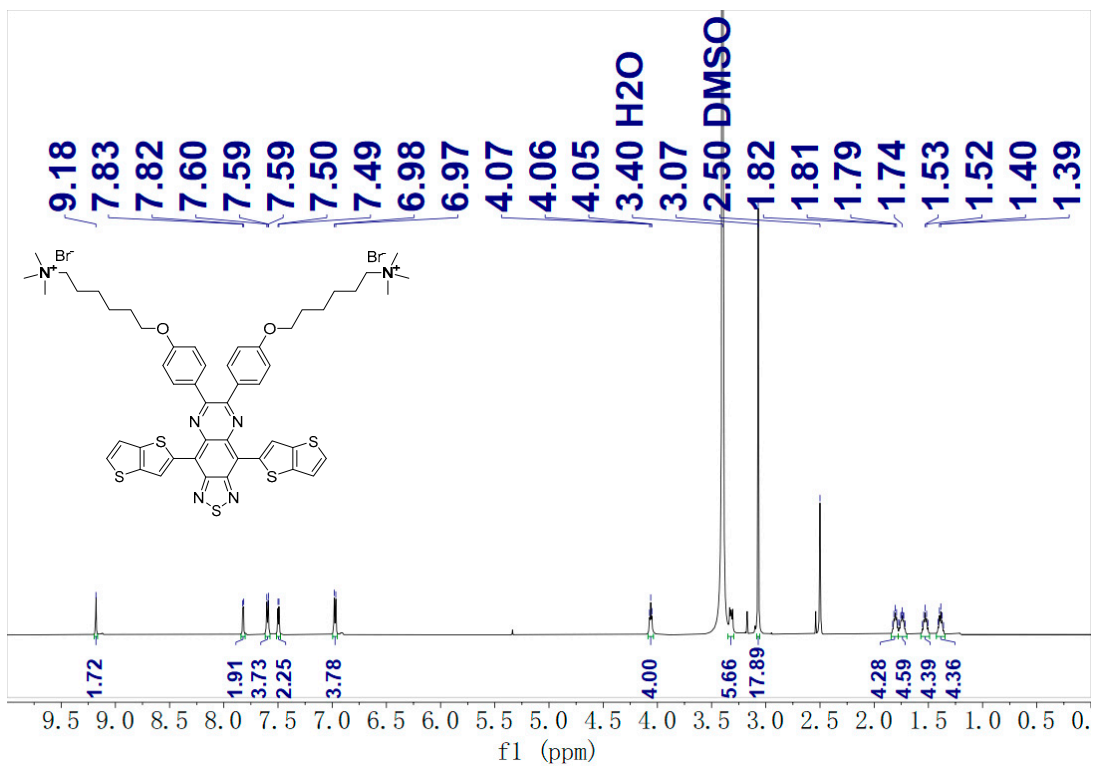


Figure S13. ^1H NMR spectrum of TTQTMA in DMSO.

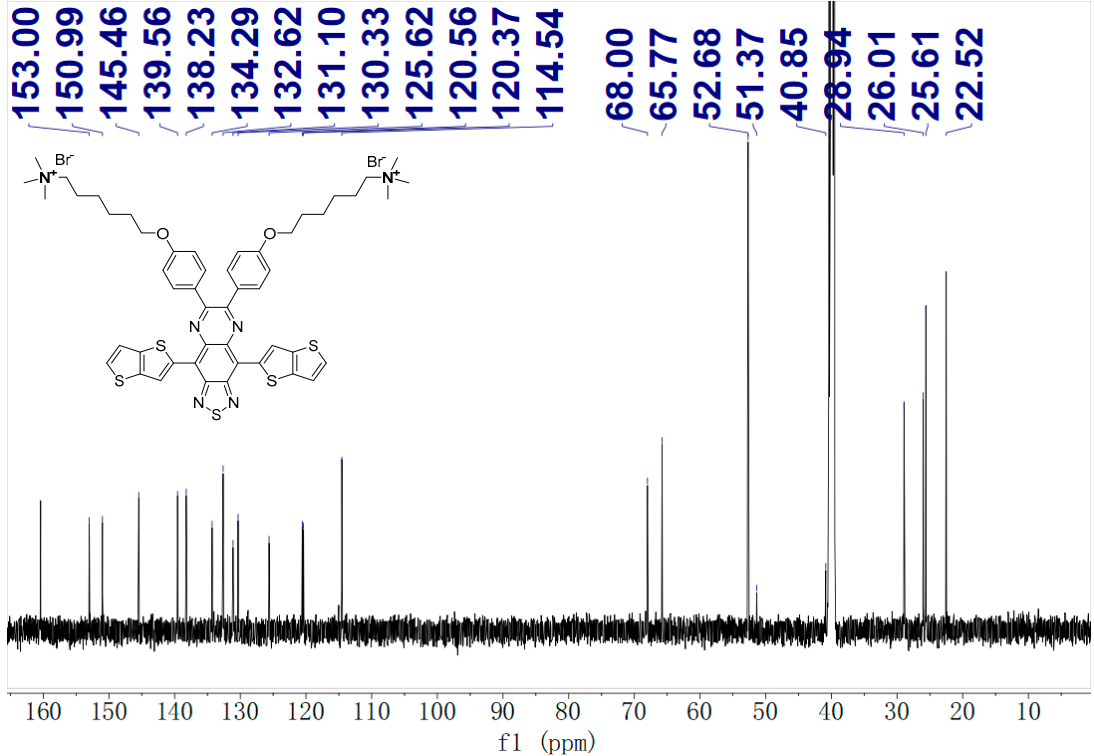


Figure S14. ^{13}C NMR spectrum of TTQTMA in DMSO.

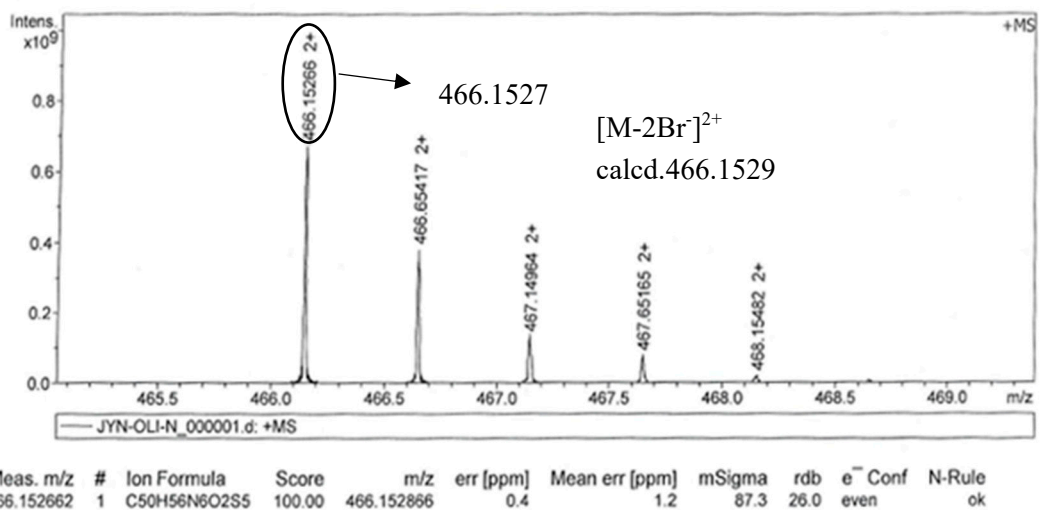


Figure S15. HRMS of TTQTMA.

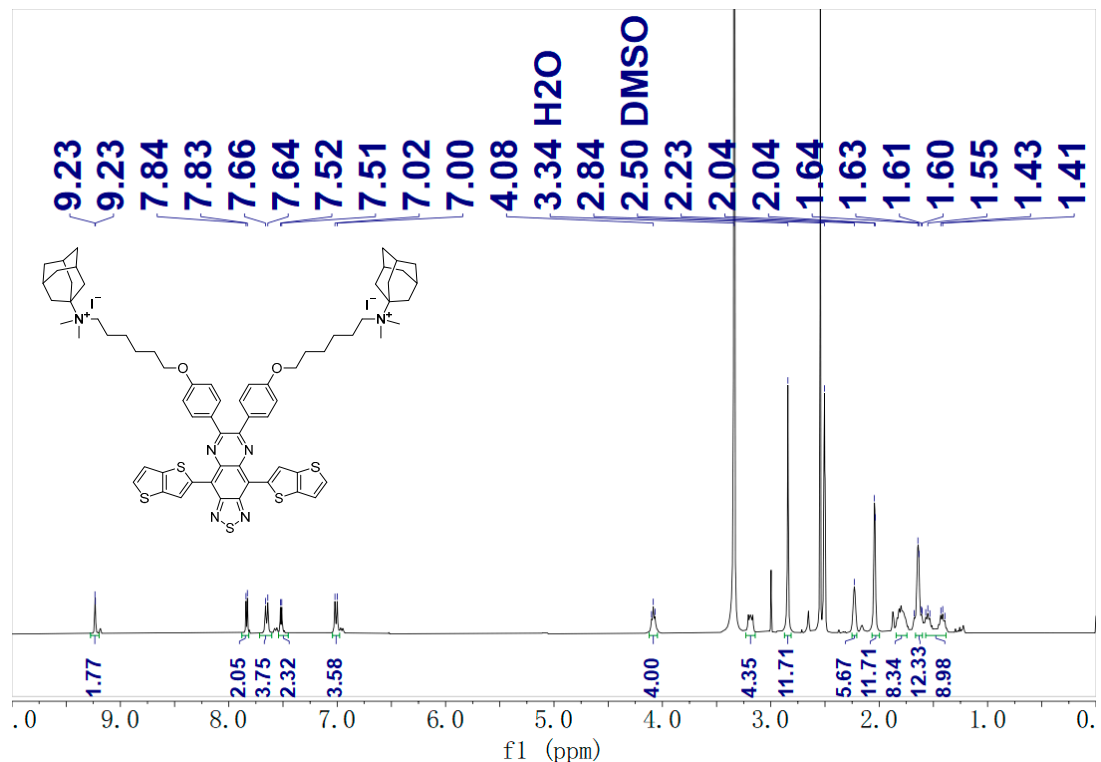


Figure S16. ^1H NMR spectrum of TTQAd in DMSO.

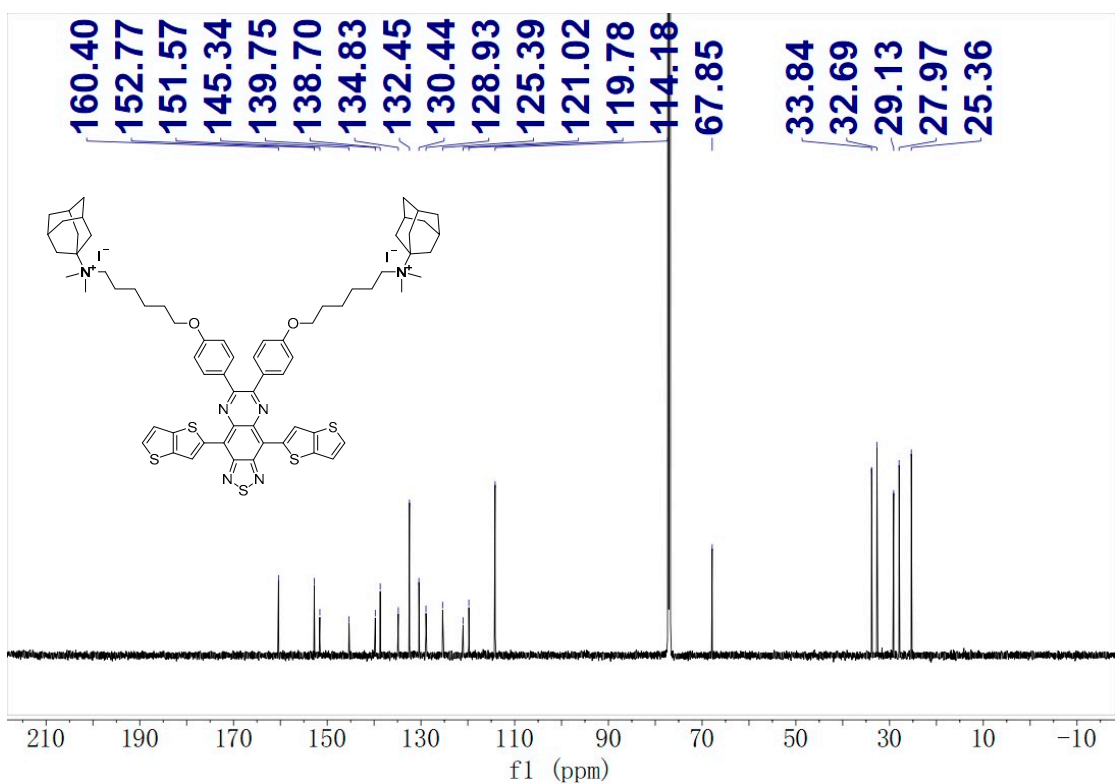


Figure S17. ^{13}C NMR spectrum of TTQAd in DMSO.

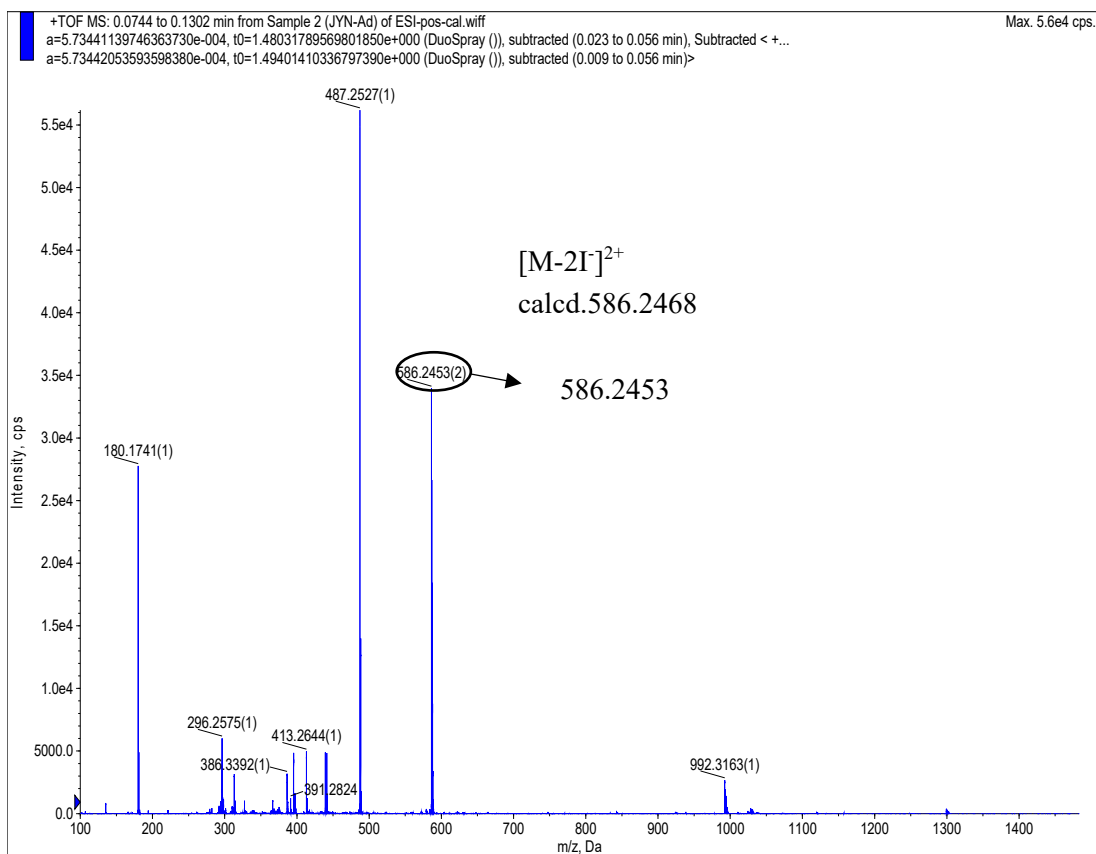


Figure S18. HRMS of TTQAd.

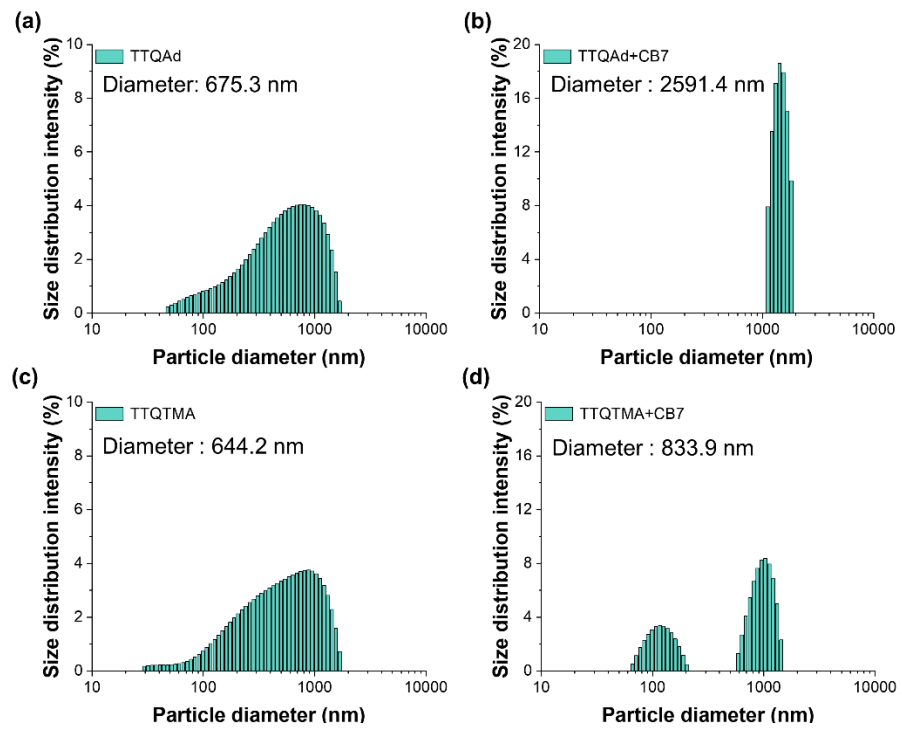


Figure S19. The hydrodynamic diameter histogram of TTQAd and TTQTMA before and after the addition of CB7. (TTQAd/TTQTMA: CB7= 1:2).

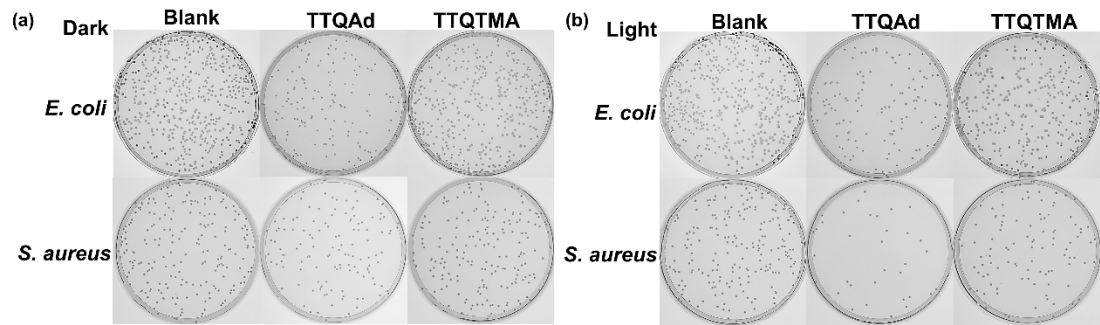


Figure S20. (a) The photographs of plate counting assay of *E. coli* and *S. aureus* treated with TTQAd/TTQTMA (20 μ M) in the dark. (b) The photographs of plate counting assay of *E. coli* and *S. aureus* treated with TTQAd/TTQTMA (20 μ M) followed by 808 nm laser irradiation (0.5 W cm^{-2} , 10 min).

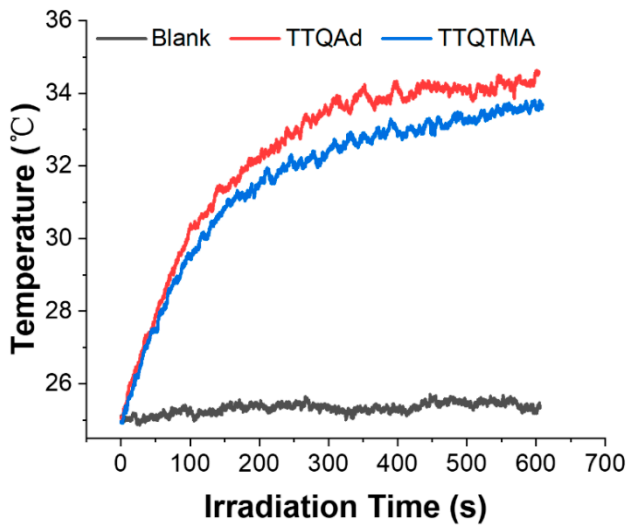


Figure S21. Photothermal conversion of TTQAd and TTQTMA in PBS (20 μM) under 808 nm laser irradiation (0.5 W cm^{-2} , 10 min).

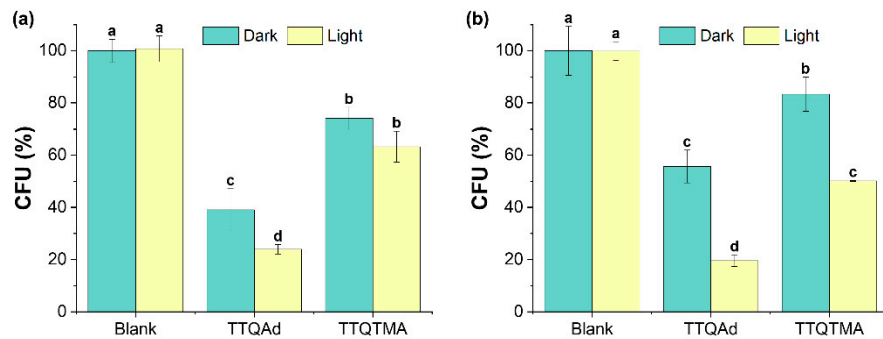


Figure S22. Bacterial viabilities of *E. coli* (a) and *S. aureus* (b) treated with TTQAd/TTQTMA (20 μM) with/without 808 nm laser irradiation (0.5 W cm^{-2} , 10 min). Different letters (a, b, c, d) in the bar graphs represent significant difference at $p < 0.05$ levels.

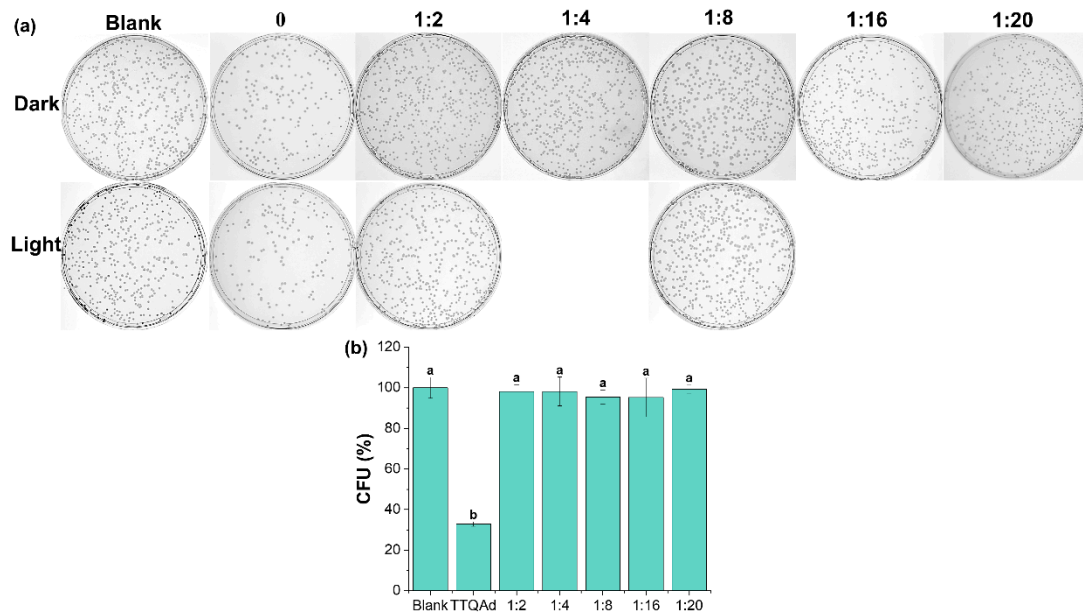


Figure S23. Photographs of *E. coli* colonies on agar plates (a) and bacterial viabilities of *E. coli* (b) treated with TTQAd before and after the addition of different amounts of CB7 with/without 808 nm laser irradiation (0.5 W cm^{-2}). [TTQAd] = 20 μM , [CB7] = 0, 40, 80, 160, 320, 400 μM . Different letters (a, b, c, d) represent significant difference at $p < 0.05$ levels.

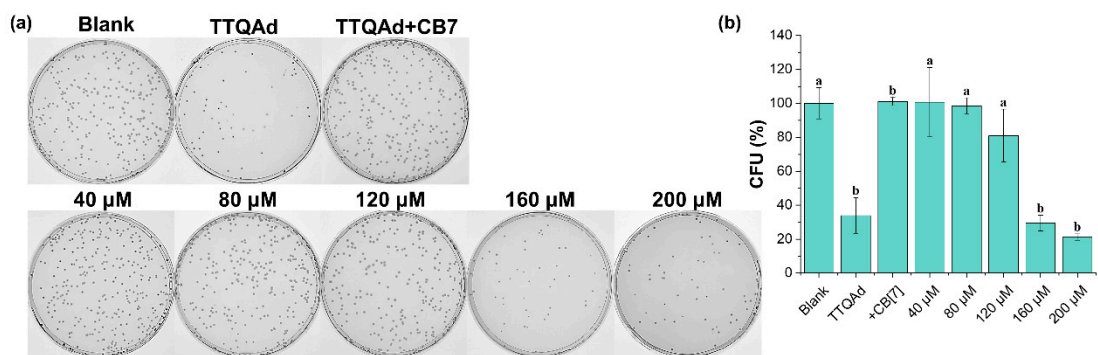


Figure S24. Photographs of *E. coli* colonies on agar plates (a) and bacterial viabilities of *E. coli* (b) treated with TTQAd-CB7 and different amounts of TMeAd. [TTQAd-CB7] = 20 μM , [TMeAd] = 0, 40, 80, 120, 160, 200 μM . Different letters (a, b) in the bar graph represent significant difference at $p < 0.05$ levels.

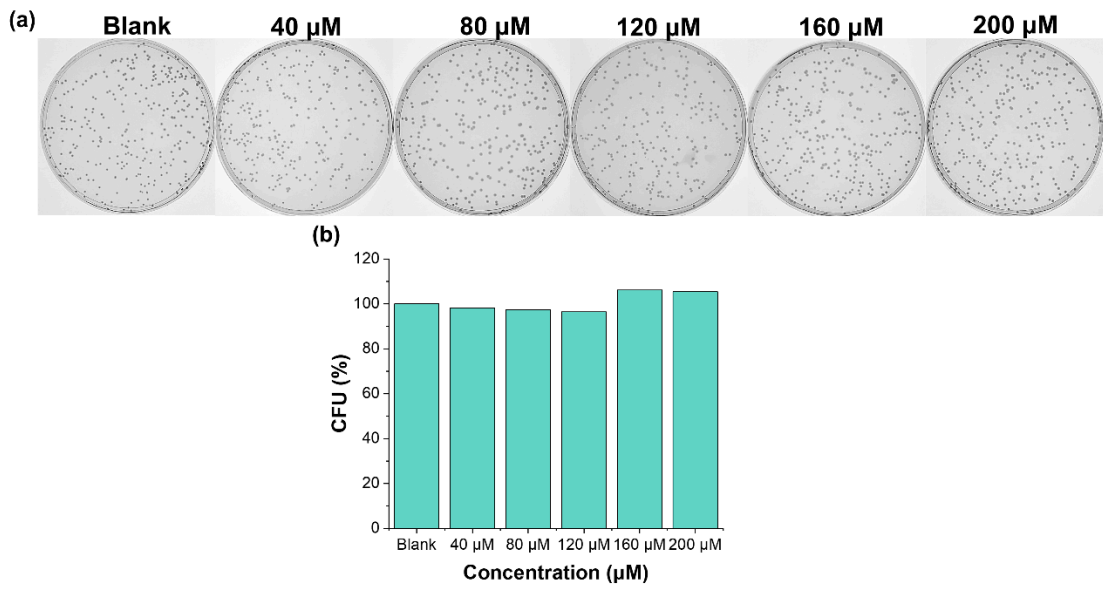


Figure S25. Photographs of *E. coli* colonies on agar plates (a) and bacterial viabilities of *E. coli* (b) treated with TMeAd. [TMeAd] = 0, 40, 80, 120, 160, 200 μ M.

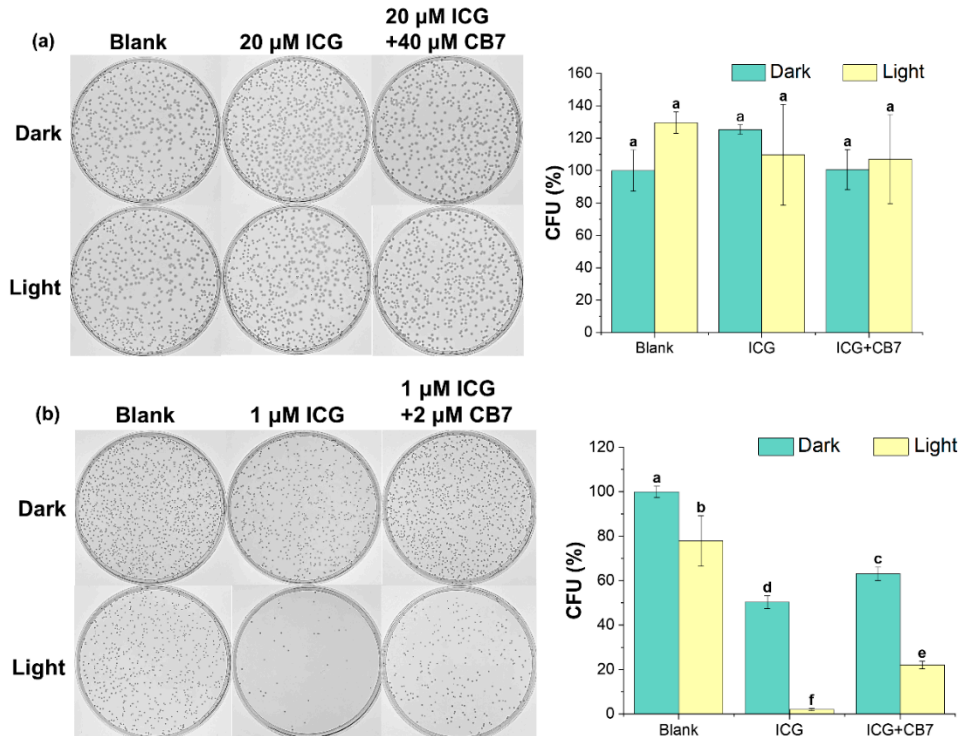


Figure S26. (a) Photographs of *E. coli* colonies on agar plates and bacterial viabilities of *E. coli* treated with ICG (20 μ M) before and after the addition of CB7 (40 μ M) with/without 808 nm laser irradiation (0.5 W cm⁻², 10 min); (b) Photographs of *S. aureus* colonies on agar plates and bacterial viabilities of *S. aureus* treated with ICG (1

μM) before and after the addition of CB7 ($2 \mu\text{M}$) with/without 808 nm laser irradiation (0.5 W cm^{-2} , 10 min); Different letters (a, b, c, d) in the bar graphs represent significant difference at $p < 0.05$ levels.

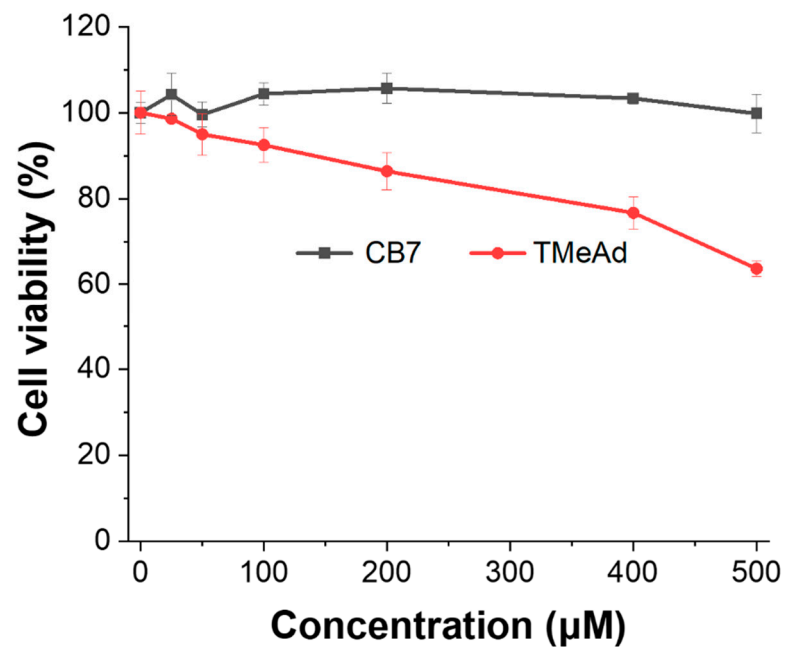


Figure S27. Cell viability after treating with CB7 and TMeAd at different concentrations in the absence of light.